NUKLEONIKA 2013;58(1):105–108

ORIGINAL PAPER

Structural and magnetic properties of the as-cast $Nd_{10}Fe_{83}Zr_1B_6$ ribbons, studied by X-ray diffraction and Mössbauer spectroscopy

Agnieszka Ceglarek, Danuta Płusa, Piotr Pawlik, Piotr Gębara

Abstract. The $Nd_{10}Fe_{83}Zr_1B_6$ alloy ribbons, prepared by melt-spinning technique, have been investigated by X-ray diffraction (XRD) and Mössbauer spectroscopy. Magnetic properties were studied by Faraday balance and vibrating sample magnetometry (VSM). The ribbon samples were produced at various surface velocities of the copper wheel from 10 m/s to 20 m/s. The XRD and Mössbauer spectra analysis have shown that the ribbons consist of the soft magnetic α-Fe, hard magnetic $Nd_2Fe_{14}B$ and disordered phases. The results showed that a uniform $Nd_2Fe_{14}B$/α-Fe nanocomposite structure with fine α-Fe grains can be obtained at an optimum velocity of the cooper roll of 20 m/s. The samples produced in these conditions had the best magnetic properties (μ_0H_C= 0.84 T, μ_0M_R = 1.05 T, μ_0M_S = 1.36 T, $(BH)_{max}$ = 160 kJ/m^3) with strong exchange coupling between the hard magnetic $Nd_2Fe_{14}B$ and soft magnetic α-Fe phases. The amorphous phase existing between grains causes an increase in the remanence and remanence ratio.

Key words: hard magnetic magnets • melt-spinning technique • Mössbauer spectroscopy • nanocomposites

Introduction

Hard magnets Nd-Fe-B, discovered in the 1980's belong to the latest generation of magnets with best magnetic properties and have been intensively studied until now [2, 3]. In recent years a great interest is focused on the so-called nanocomposite magnets consisting of α-Fe/$Nd_2Fe_{14}B$ phases for which the grain diameters are lower than 40 nm. It is well known that the addition of Zr improve the energy product and squareness of the hysteresis loop in two-phase nanocomposite magnets. This is due to the fact that the admixture of Zr or Nb retards the growth of crystalline phases [7, 10]. The raw material for nanocomposite magnets are ribbons produced by the melt-spinning technique [1, 4, 8, 9]. The characteristic feature of nanocomposite magnets which distinguish them from magnets with larger grains, is the remanence enhancement due to the exchange interactions between the soft and hard magnetic grains. Majority of the previous studies were concentrated around to the remanence enhancement via the exchange coupling between neighboring α-Fe and $Nd_2Fe_{14}B$ grains. But some authors suggest that the disordered intergranular phase existing at grain boundaries may improve the exchange coupling by reducing the effective anisotropy constant and thus increasing the exchange interaction length [5, 6, 11]. The volume fraction of the disordered phase can be modified by changes in rapid solidification processing conditions. Therefore, in the present work the influence of the phase constitution and volume fraction of constituent phases on the magnetic properties,

A. Ceglarek✉, D. Płusa, P. Pawlik, P. Gębara
Technical University of Częstochowa,
Institute of Physics,
19 Armii Krajowej Ave., 42-200 Częstochowa, Poland,
Tel./Fax: +48 34 325 0795,
E-mail: a.ceglarek@go2.pl

Received: 11 June 2012
Accepted: 25 October 2012

of the $Nd_{10}Fe_{83}Zr_1B_6$ alloy ribbons obtained at various surface velocities were studied.

Experimental

The $Nd_{10}Fe_{83}Zr_1B_6$ alloy ribbons of various thicknesses were prepared by arc-melting of the high-purity elements under an Ar atmosphere. The ingot sample was re-melted several times in order to ensure homogeneity of its structure. The ribbons of various thicknesses from 35 μm to 50 μm, were melt-spun at various surface velocities, from 10 m/s to 20 m/s. The pressure inside the chamber was $0.4*10^5$ Pa. The phase constitution was examined using a Bruker D8 Advance X-ray diffractometer equipped with a Lynx Eye semiconductor detector and CuK_α radiation. The hysteresis loops were measured at room temperature using a LakeShore 7307 vibrating sample magnetometer at external magnetic fields up to 2 T. From the major hysteresis loops, the magnetic parameters, i.e.: coercivity μ_0H_C, remanence μ_0M_R, saturation magnetization μ_0M_S, and maximum magnetic energy product $(BH)_{max}$ were determined. The thermomagnetic curves M(T) were obtained using the Faraday balance operating at a magnetic field of 0.87 T and temperature range from 300 K to 850 K with a heating rate of 10 K/min. The Mössbauer studies were performed using a Polon Mössbauer spectometer with constant acceleration of a ^{57}Co source embedded within a Rh matrix and activity of 100 mCi. The spectra analysis was performed using WinNorms for the Igor 3.0 package.

Results and discussion

The X-ray diffraction patterns obtained for the $Nd_{10}Fe_{83}Zr_1B_6$ alloy ribbons in the as-cast state, melt-spun at various velocities of the copper wheel are presented in Fig. 1. It was shown that the increase of velocity of the copper wheel from 10 m/s to 20 m/s, resulted in an increase of intensities of peaks corresponding to the hard magnetic $Nd_2Fe_{14}B$ phase. Furthermore, for all investigated samples the presence of XRD reflexes originating from the soft magnetic α-Fe phase was revealed. The broadening of the peaks shown for the samples produced at higher velocities suggests a decrease of the grain sizes of constituent phases.

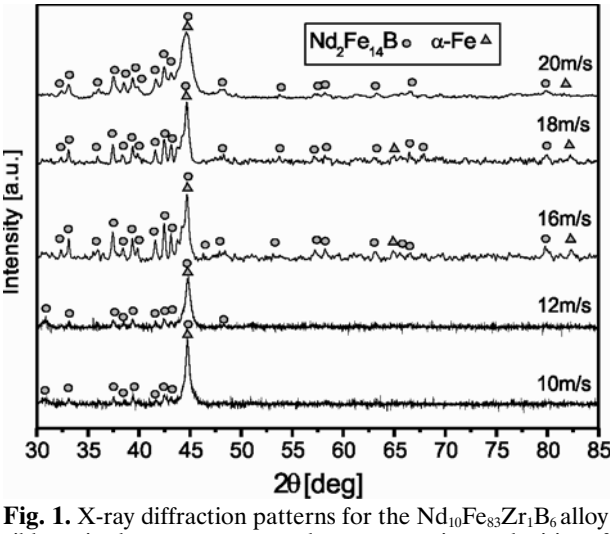

Fig. 1. X-ray diffraction patterns for the $Nd_{10}Fe_{83}Zr_1B_6$ alloy ribbons in the as-cast state melt-spun at various velocities of the copper wheel.

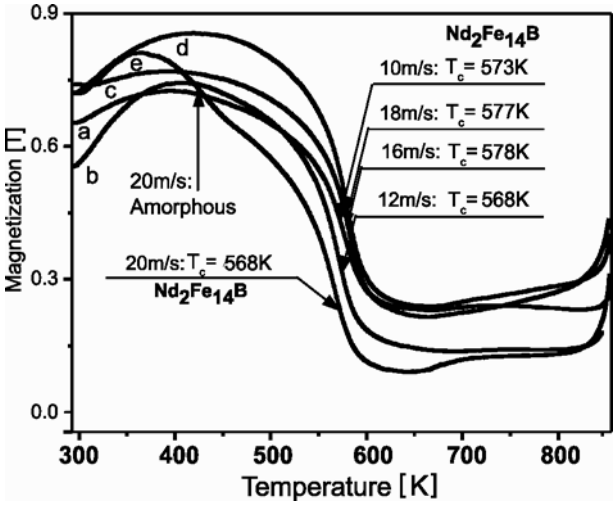

Fig. 2. Thermomagnetic curves M(T) for ribbons of the $Nd_{10}Fe_{83}Zr_1B_6$ alloy in as-cast state produced at (a) 10 m/s, (b) 12 m/s, (c) 16 m/s, (d) 18 m/s, (e) 20 m/s.

The average grain size of the $Nd_2Fe_{14}B$ phase was estimated using Scherrer's method from the broadening of the diffraction peaks, and for the sample produced at 20 m/s reaches 40 nm.

The thermomagnetic curves M(T) measured in the temperature range from 293 K to 853 K are presented in Fig. 2. The rise of magnetic moment at temperatures lower than 400 K is due to a significant decrease of the magnetic anisotropy constants of the hard magnetic phase, thus leading to easier ordering of the magnetic moments. In higher temperature range, for ribbons produced at velocities up to 18 m/s, a single stage decrease of magnetization around temperate corresponding to the Curie point T_C of the $Nd_2Fe_{14}B$ phase was observed. However, for ribbon melt-spun at 20 m/s, the two stage M(T) curve was measured. Taking into account the XRD studies, this suggests the presence of a large amount of the amorphous phase in the alloy composition, for which T_C is lower than that for the $Nd_2Fe_{14}B$ phase. Due to the limited range of the experimental method, the ferro- to paramagnetic phase transition for the α-Fe phase was not detected.

Mössbauer spectra obtained for samples produced at various surface velocities of the copper wheel from 10 m/s to 20 m/s are shown in Fig. 3(a–e). The ribbons were crushed to powder to produce representative samples for the Mössbauer spectra measurements. Thus the approach of a thin absorber was used in the fitting model. In the fitting procedure the presence of the hard magnetic $Nd_2Fe_{14}B$ was represented by six sextets. This is due to the existence of six non-equivalent Fe atom positions in the unit cell of the hard magnetic phase. Relative intensities of those sextets were chosen as 4:4:2:2:1:1, according to the ratio of Fe occupancy corresponding to Fe atom sites denoted in the Wyckoff notation as $16k_1$, $16k_2$, $8j_1$, $8j_2$, $4c$ and $4e$. Furthermore, the presence of α-Fe phase was represented by one Zeeman line. For the best fitting, additional two lines

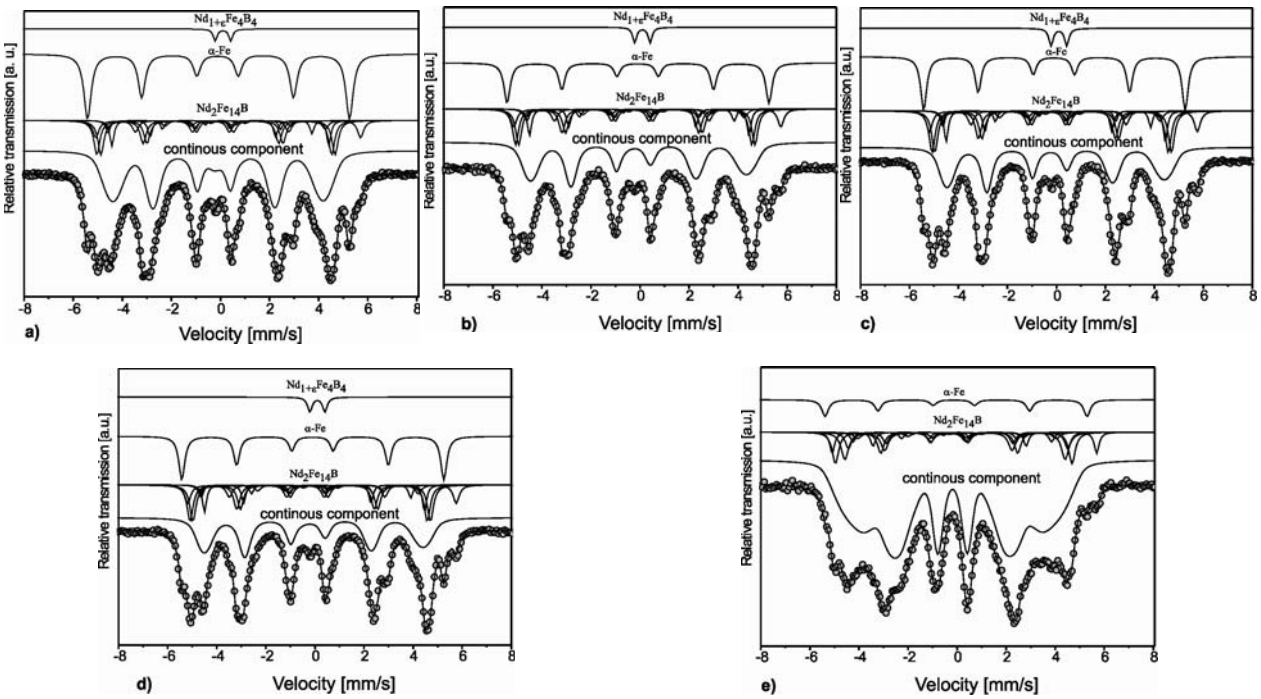

Fig. 3. The Mössbauer spectra for ribbons produced at (a) 10 m/s, (b) 12 m/s, (c) 16 m/s, (d) 18 m/s, (e) 20 m/s.

Table 1. The weight fractions of constituent phases of the $Nd_{10}Fe_{83}Zr_1B_6$ alloy ribbons produced at various velocities of the copper wheel

Sample (m/s)	$Nd_2Fe_{14}B$ V (wt.%)	α-Fe V (wt.%)	$Nd_{1+\varepsilon}Fe_4B_4$ V (wt.%)	Disordered phase V (wt.%)
10	33.4	18.0	1.9	46.7
12	46.0	12.5	3.4	38.2
16	48.7	14.7	3.8	32.8
18	48.0	13.4	3.9	34.7
20	23.3	3.0	–	73.7

were incorporated. The one doublet corresponds to the presence of the paramagnetic $Nd_{1+\varepsilon}Fe_4B_4$ phase that was not detected by XRD. Due to the application of rapid solidification technique for preparation of the samples, the existence of some disordered phases in the investigated samples was also expected. Therefore, for complete fitting a broad component corresponding to the hyperfine field distribution was also used.

The Mössbauer spectra analysis allowed to determine weight fractions of constituent phases. These values are collected in Table 1.

It was shown that for all investigated ribbons the major crystalline phase formed during rapid solidification is the hard magnetic $Nd_2Fe_{14}B$. In case of the ribbons melt-spun at velocities not higher than 18 m/s, a similar fractions of disordered phase (more than 30 wt.%) were determined, while α-Fe takes above 10 wt.%. The spectra analysis revealed also some traces of the paramagnetic $Nd_{1+\varepsilon}Fe_4B_4$ phase in the melt-spun ribbon. A significant change of the phase constitution was observed for the ribbon obtained at the velocity of 20 m/s, where only ~23 wt.% of the $Nd_2Fe_{14}B$ phase, and more than 70 wt.% of the disordered phase was determined. Furthermore, the hyperfine field distributions corresponding to the disordered phase suggest significant changes of their chemical composition together with the velocity of the copper roll. The hyperfine field distributions for continuous component of the resolved spectra measured for ribbons produced at 10 m/s and 20 m/s are shown in Fig. 4. Similar distributions

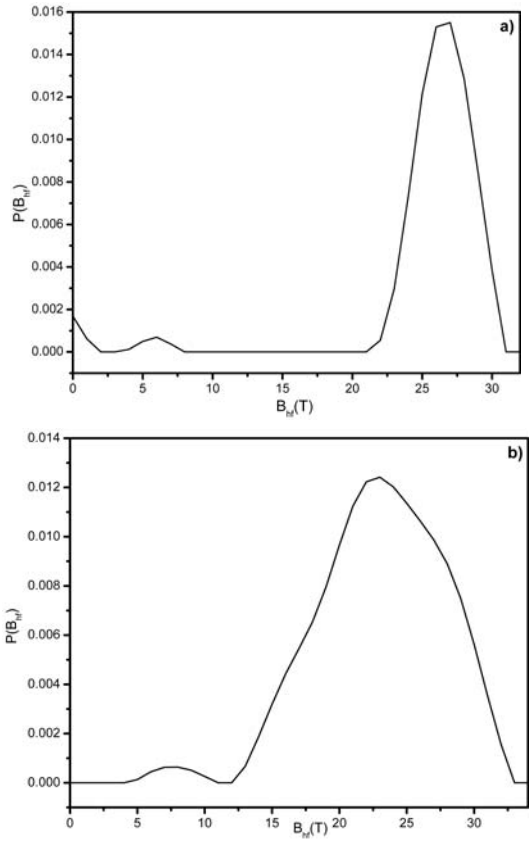

Fig. 4. The hyperfine field distributions corresponding to the continuous components of the Mössbauer spectra representing disordered component of ribbons obtained at 10 m/s (a) and 20 m/s (b).

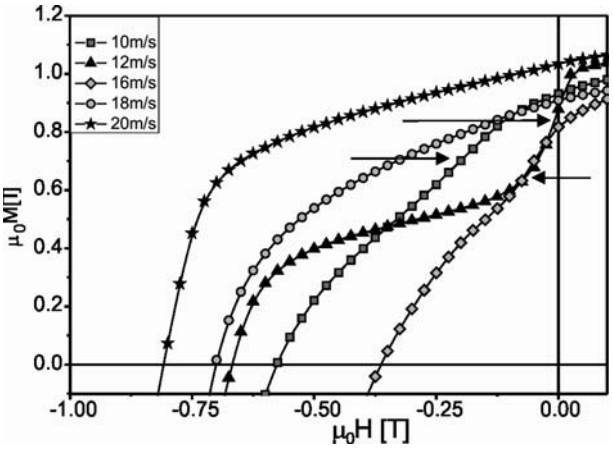

Fig. 5. Demagnetization curves for ribbons produced at 10 m/s, 12 m/s, 16 m/s, 18 m/s, 20 m/s in the as-cast state (arrows correspond to the kink).

and corresponding continuous components were obtained for specimens produced at velocities lower than 18 m/s.

The distribution determined for ribbon produced at 20 m/s is broad and asymmetric with a maximum around 22 T. Such a distribution and fraction of disordered phase indicates that grains of crystalline phases are dilute within the amorphous matrix. In case of ribbons melt-spun at velocities lower than 18 m/s the hyperfine field distributions are narrow with its maximum around 27 T. According to suggestion reported in [8] the high remanence of sample obtained at 20 m/s can originate from the existence of intergranular phases. The presence of such phases can cause the reduction of effective anisotropy constant $<K>$ and increasing the exchange length $L_{ex} = \sqrt{A/\langle K \rangle}$, where A is the exchange constant. The demagnetization curves for the obtained ribbons are shown in Fig. 5.

The improved magnetic properties were obtained at a velocity between 18 m/s and 20 m/s ($\mu_0 H_C$= 0.84 T, $\mu_0 M_R$ = 1.05 T, $\mu_0 M_S$ = 1.36 T, $(BH)_{max}$ = 160 kJ/m^3). Application of lower velocities results in greater grain size of the nanocrystalline phase, which, in turn, allows easier demagnetization of the sample and weakens the exchange coupling between magnetically soft and magnetically hard grains. The effect is clear for samples produced at velocities 10 m/s, 12 m/s, 16 m/s where the demagnetization curve shape (clear kink) can indicate the lack of the exchange coupling characteristic of multiphase materials. The demagnetization curve for the remaining samples are smooth and single stage which indicates strong exchange coupling between magnetic hard and magnetic soft phases and have a high remanence ratio M_R/M_S equal to 0.8. It is interesting to note that quite good magnetic properties ($\mu_0 H_C$ = 0.84 T, $\mu_0 M_R$ = 1.05 T) were obtained for only partially crystallized sample suggesting that the disordered intergranular phases can increase the exchange coupling.

Conclusions

- The $Nd_{10}Fe_{85}Zr_1B_6$ ribbons obtained at the wheel velocities from 10 m/s to 20 m/s in as-cast state are partially crystalline and consist of the hard $Nd_2Fe_{14}B$, soft α-Fe and dissordered phases.
- The calculated Mössbauer spectra fit well to the experimental ones if they were decomposed into six Lorentzian sextets corresponding to six magnetically non-equivalent position of the Fe atom in a unit cell of hard $Nd_2Fe_{14}B$ phase, one sextet corresponding to α-Fe, one component with hyperfine field distribution corresponding to the disordered NdFeB phase and one dublet corresponding to the paramagnetic $Nd_{1+\varepsilon}Fe_4B_4$ phase (for ribbons melt-spun at velocities not higher than 18 m/s).
- In case of the ribbons melt-spun at velocities not higher than 18 m/s, the disordered phase has a similar volume fraction (above 30 wt.%), while α-Fe takes above 10 wt.%.
- The ribbons obtained at 20 m/s consist of more than 70 wt.% of disordered phase and have the best magnetic parameters, the remanence ratio and good hysteresis loop squareness.
- The remanence enhancement results not only from the direct exchange coupling between fine $Nd_2Fe_{14}B$ and α-Fe grains, but from exchange coupling via the layers of disordered phases surrounding the crystalline grains.

References

1. Bauer J, Seeger M, Zern A, Kronmüller H (1996) Nanocrystalline FeNdB permanent magnets with enhanced remanence. J Appl Phys 80:1667–1673
2. Betancourt RJI (2002) Nanocrystalline hard magnetic alloys. Rev Mex Fis 48:283–289
3. Croat JJ, Herbst JF, Lee RW, Pinkerton FE (1984) Pr-Fe and Nd-Fe-based materials: A new class of high-performance permanent magnets. J Appl Phys 55:2078 (5 pp)
4. Hirosawa S, Shigemoto Y, Miyoshi T, Kanekiyo H (2003) Direct formation of $Fe_3B/Nd_2Fe_{14}B$ nanocomposite permanent magnets in rapid solidification. Scripta Mater 48:839–844
5. Kobayashi T, Yamasaki M, Hamano M (2000) Mössbauer study on intergranular phases in the bcc-Fe/NdFeB nanocomposite alloys. J Appl Phys 87:6579–6581
6. Li S, Gu B, Bi H *et al*. (2002) Role of amorphous grain boundaries in nanocomposite NdFeB permanent magnets. J Appl Phys 92:7514–7518
7. Wang C, Yan M, Li Q (2008) Effects of Nd and B contents on the thermal stability of nanocomposite $(Nd,Zr)_2Fe_{14}B$/α-Fe magnets. Mat Sci Eng B 150:77–82
8. Wu YQ, Ping DH, Hono K, Hamano M, Inoue A (2000) Microstructural characterization of an alpha-$Fe/Nd_2Fe_{14}B$ nanocomposite magnet with a remaining amorphous phase. J Appl Phys 87:8658–8665
9. Wu YQ, Ping DH, Xiong XY, Hono K (2002) Magnetic properties and microstructures of α-$Fe/Nd_2Fe_{14}B$ nanocomposite microalloyed with Zr. J Appl Phys 91:8174–8176
10. Xiaoqian B, Jie Z, Wei L, Xuexu G, Shouzeng Z (2009) Influence of zirconium addition on microstructure, magnetic properties and thermal stability of nanocrystalline Nd12.3Fe81.7B6.0 alloy. J Rare Earths 27:843–847
11. Yamasaki M, Hamano M, Kobayashi T (2002) Mössbauer study on the crystallization process of α-$Fe/Nd_2Fe_{14}B$ type magnet alloy. Mater Trans 43:2885–2885